KADET-BASED ONE-COMPONENT BEAM MODEL FOR THE SIMULATION OF CYCLIC LATERAL RESPONSE OF URM WALLS

K.G. Megalooikonomou[1]

[1] Hellenic Open University, School of Science and Technology, Parodos Aristotelous 18, 26335 Patras, Greece, std153412@ac.eap.gr

Abstract: *The one-component beam model consists of a linear elastic element connected in series with a rigid-plastic linear hardening spring at each end (concentrated or lumped plasticity element). According to the new Greek Regulation for Valuation and Structural Interventions for Masonry (KADET) common in-plane failure modes of an unreinforced masonry (URM) pier can be combined taking into account their minimum envelope leading to a single failure mode interaction plastic spring for the shear span of each masonry frame element similar to the aforementioned one-component model. The moment or shear (accordingly through moment's division with the shear span length) -axial load interaction of the URM pier is taken into account in the aforestated minimum envelope although it is not included in the original formulation of the latter beam element. Based on the above-mentioned approach and on the results from the literature of an extensive experimental programme that included standard material tests and quasi-static cyclic tests on hollow clay brick URM walls subjected to horizontal and axial loads, a MATLAB simulation code is developed. It is evident from the correlation with the latter experimental results that the model can capture adequately the initial stiffness, failure mode and maximum lateral strength under cyclic action of URM walls and could be further extended and adopted to the equivalent frame modelling of URM buildings based on KADET.*

1. Introduction

Modelling masonry structures is still an open issue for seismic engineers. The reason for this is attributed to the complexity of masonry mechanical behaviour along with the fact of a great variability in structural types and masonry constituent materials. Nowadays, such structures represent a great part of the cultural heritage of the Mediterranean area and therefore there is an urgent need of seismic assessment and retrofit of historical masonry buildings (Megalooikonomou et al 2018, Pittore et al 2018).

Nonlinear static procedures and equivalent-frame models (Bracchi et al 2015) are widely used in practical engineering applications due to their simplicity and adequate computational cost (DeJong 2009). A detailed discussion of the advantages of employing such models in comparison with other methodologies can be found in numerous studies (Calderini et al 2009, Marques and Lourenco 2011, Ambra et al 2016, Magenes and Calvi 1996, Lagormarsino et al 2013).

Computer programs employing equivalent frame modelling approach allow the analysis of relatively complex buildings with significantly lower computational effort compared to more demanding approaches, such as finite element, applied element and discrete element methods, making them suitable for practice engineering purposes (Cattari et al. 2021, 2022). However, nonlinear beam models available in commercial structural analysis software cannot explicitly address the principal failure modes of URM piers observed during experiments (e.g. rocking/toe crushing, bed joint sliding, and diagonal tension). Nowadays, to address this shortcoming, many macro-elements have been developed to replace the plastic hinge and nonlinear beam elements within the equivalent frame model. This approach provides rotational, shear, and axial springs in series and was first put forth by Kabeyasawa (1982) for the analysis of reinforced concrete shear walls and later modified by James and Kunnath (1994). The principal alteration of these models required for applications to URM piers was the addition of two shear springs at the top and bottom of the macro-element to account for bed joint sliding deformation in these regions. The macro-elements have three degrees of freedom at each end and thus can be used within an equivalent frame model for the analysis of URM walls (Chen et al. 2008).

However, this study is focused on the proposal of a one-component beam model for the simulation of cyclic lateral response of unreinforced masonry (URM) walls based on the new Greek Regulation for Valuation and Structural Interventions for Masonry (KADET 2022). According to KADET, common in-plane failure modes of an URM pier can be combined taking into account their minimum envelope leading to a single failure mode interaction plastic spring for the shear span of each masonry frame element similar to the aforementioned one-component model. The moment or shear (accordingly through moment's division with the shear span length) -axial load interaction of the URM pier is taken into account in the aforestated minimum envelope although it is not included in the original formulation of the latter beam element.

In the following Sections the proposed beam formulation for equivalent frame modelling of URM piers will be described thoroughly and its numerical results will be correlated to experimental results from the literature.

2. Regulation for valuation and structural interventions for masonry (KADET)

In the subsections below the in-plane strength assessment of a URM pier through KADET and its implications are described in detail.

2.1. In-plane flexural strength of URM pier

The shear capacity of a URM pier controlled by flexure under the presence of an axial load is given by the following equation according to KADET:

$$V_f = \frac{L}{2}\frac{\mathrm{N}}{H_0}(1 - 1.15 \cdot v_d) \tag{1}$$

where:

- L: the horizontal in-plane dimension (length) of the URM pier
- H_0: the shear span of the pier
- N: the axial load of the pier
- $v_d = N / (L\ t\ f_d)$
- t : the thickness of the pier
- f_d : the compression strength of the wall

2.2. In-plane shear strength due to sliding of URM pier

The shear capacity of a URM pier controlled by shear under the presence of an axial load is given by the following equation according to KADET:

$$V_{vs} = f_{vs} \cdot L' \cdot t \tag{2}$$

where:

- L': the depth of the compression zone of the URM pier
- $f_{vs} = f_{vm0} + 0.4(N / L't) \leq 0.065\ f_b$: the mean shear strength of the URM pier that takes into account the presence of the axial load
- N: the axial load of the pier
- t : the thickness of the pier
- f_{vm0} : the mean shear strength of the URM pier without the presence of the axial load
- f_b : the compression strength of the masonry wall unit

2.3. In-plane shear strength due to diagonal tension of URM pier

The shear cracking strength due to diagonal cracking parallel to the principal compressive stresses and perpendicular to the principal tensile stresses, is given by the following equation according to KADET:

$$V_{vt} = f_{vt} \cdot L \cdot t \quad (3)$$

where:

- L: the horizontal in-plane dimension (length) of the URM pier
- $f_{vt} = \sqrt{[f_{wtd}(f_{wtd}+v_d f_d)]}$: the shear cracking stress of the URM pier
- f_{wtd}: the mean tensile masonry strength
- N: the axial load of the pier
- $v_d = N / (L\ t\ f_d)$
- t : the thickness of the pier
- f_d : the compression strength of the wall

2.4. Minimum envelope for in-plane strength assessment of URM pier

Figure 1 plots descriptively all the envelopes of each strength (shear or flexural) defined by the above equations in the previous subsections and by taking the minimum strength of the above quantities, the final strength V_{Rd} of the URM pier is defined for a specific applied axial load as it is depicted in the Figure 1 below. Thus, the shear-axial load interaction for the URM pier under study is taken into account. Finally, by multiplying the final strength in terms of shear with the shear span of the pier, the plastic moment of a single failure mode interaction plastic spring of each end of the masonry frame element modelled here though the one-component beam model is defined.

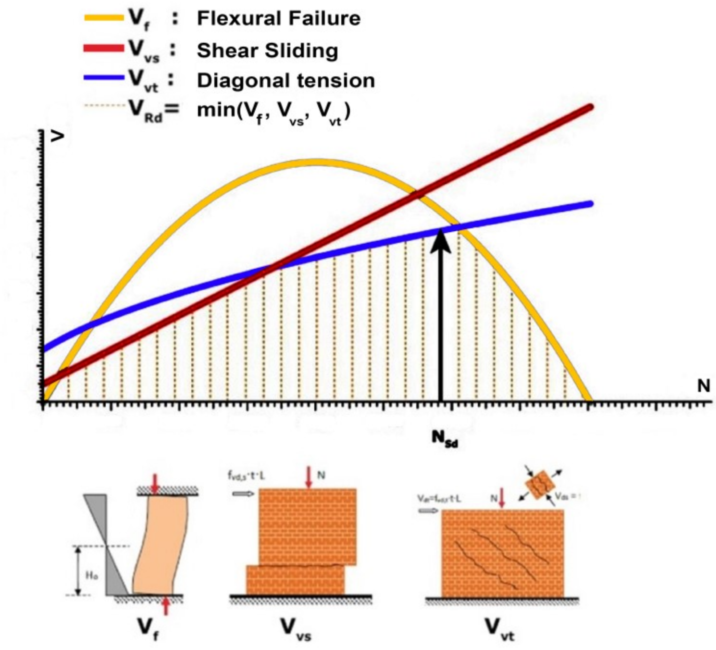

Regulation for Valuation and Structural Interventions for Masonry (KADET)

Figure 1. Minimum envelope for in-plane strength assessment of URM pier according to KADET

3. One-component beam model

An elasto-plastic frame structure was analyzed by placing a rigid plastic spring at the location where yielding is expected. The part of the member between the two rigid plastic springs remains perfectly elastic as it is shown in the Figure 2 below. This one-component model was generalized by Giberson (1967,1969). A major advantage of the model is that inelastic member-end deformation depends solely on the moment acting at the end so that any moment-rotation hysteretic model can be assigned to the spring. Despite rational criticisms against this simple model, the performance of the one-component model is expected to be reasonably good for a relatively low-rise frame structure, in which the inflection point of a pier locates close to mid-height.

The state determination of a model in series with a single unknown is straightforward. In one-component beam model there are two unknowns, the basic forces q_2 and q_3. This makes the state determination more complicated but it is simplified by the fact the constitutive law for the nonlinear component is rigid plastic, linear hardening which obviates the need for an iteration at the component level as the Figure 2 below illustrates. An iteration at the element is, however, still necessary.

The only input needed for modelling a URM pier with one-component frame model is the elastic properties of the pier *EA* and *EI* (*E*: modulus of elasticity, *A*: area of the URM pier section, *I*: moment of inertia of URM pier section) and the plastic moments M_p of each rigid plastic spring at the ends defined in the previous section. In the next section the cyclic response of this one-component beam model will be defined excluding the hardening (isotropic or kinematic) response for modeling of URM masonry walls.

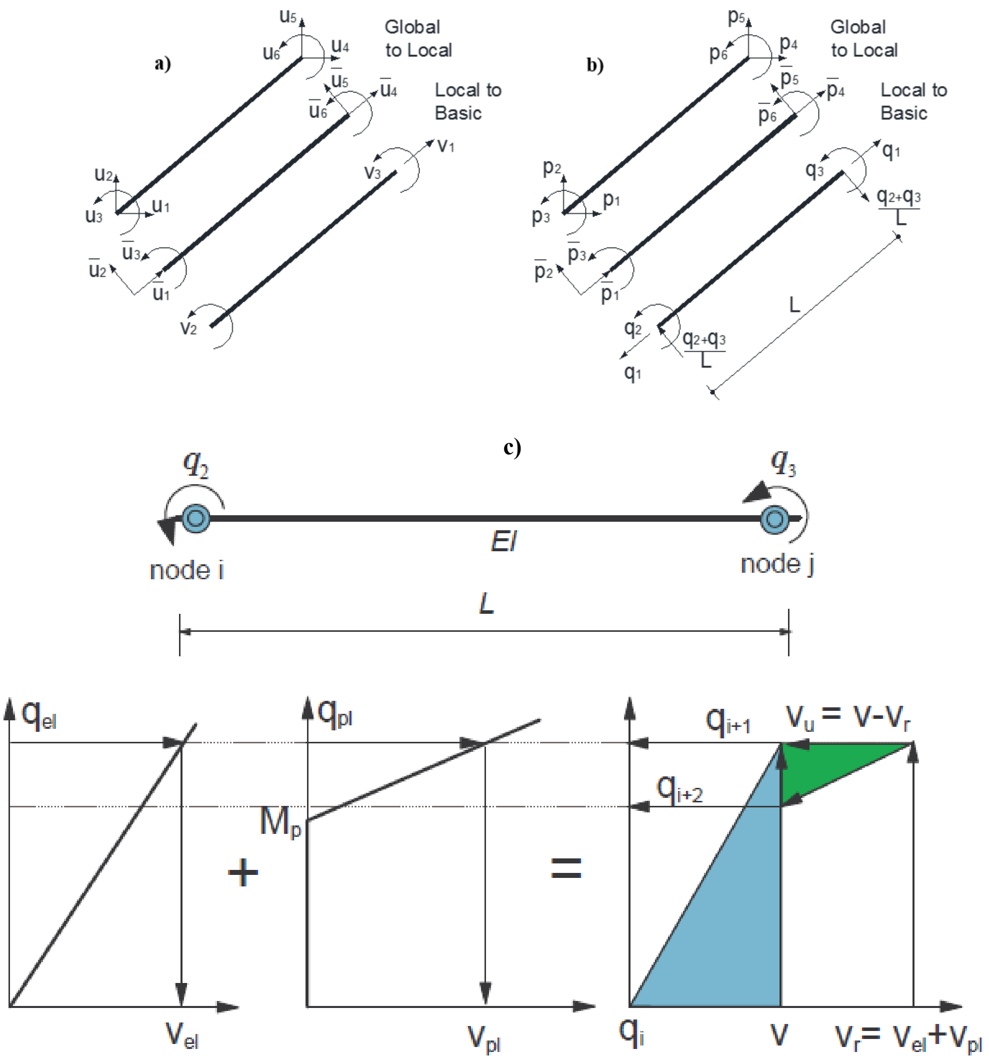

Figure 2. Beam a) displacements and b) forces in global, local and basic reference systems and c) the corresponding state determination of one-component beam model (Filippou and Fenves 2004)

4. Path-dependent plasticity for element response

For a linear elastic, perfectly plastic beam with a non-smooth multi-surface plasticity, the equilibrium, compatibility and constitutive relation of elastic component along with the yield function are given in the following equations based on Figures 2 and 3 (Filippou and Fenves 2004, Simo and Hughes 1998, Hughes 2000):

$$\text{Equilibrium: } q = q_e = q_p \tag{4}$$

$$\text{Compatibility: } v = v_e + v_p \text{ with } v_p = \begin{pmatrix} 0 \\ v_{p2} \\ v_{p3} \end{pmatrix} \tag{5}$$

$$\text{Constitutive relation of elastic component: } q = k_e \cdot v_e = k_e \cdot (v - v_p) \tag{6}$$

$$\text{Yield function: } f_1(q_2, q_3) = |q_2| - M_{pi} \leq 0 \text{ for node i} \tag{7}$$

$$\text{Yield function: } f_2(q_2, q_3) = |q_3| - M_{pj} \leq 0 \text{ for node j} \tag{8}$$

There are now two independent yield surfaces, one for node *i* and one for node *j*. They can be written in a more compact form by recalling that |x| = sign(x)x:

$$f_1(q_2, q_3) = sign(q_2)(q_2) - M_{pi} \leq 0 \tag{9}$$

$$f_2(q_2, q_3) = sign(q_3)(q_3) - M_{pj} \leq 0 \tag{10}$$

Taking the derivative:

$$\frac{\partial f_1}{\partial \boldsymbol{q}} = \begin{pmatrix} 0 \\ sign(q_2) \\ 0 \end{pmatrix} = n_2 \tag{11}$$

$$\frac{\partial f_2}{\partial \boldsymbol{q}} = \begin{pmatrix} 0 \\ 0 \\ sign(q_3) \end{pmatrix} = n_3 \tag{12}$$

With the definition $n = [n_2 \quad n_3]$ and $\frac{\partial f}{\partial \boldsymbol{q}} = n^T$ the yield conditions can be rewritten:

$$f(q_2, q_3) = n^T q - q_{pl} \leq 0 \text{ with } q_{pl} = \begin{pmatrix} 0 \\ M_{pi} \\ M_{pj} \end{pmatrix} \tag{13}$$

The flow rule for non-smooth plasticity is given below:

$$\text{Flow rule: } \dot{v}_p = n_2\beta_2 + n_3\beta_3 = n\beta \text{ iff } f(q_2, q_3) = n^T q - q_{pl} = 0 \tag{14}$$

$$\text{Kuhn-Tucker conditions: } \beta_k \geq 0 \text{ and } f_k \leq 0 \text{ and } \beta_k f_k = 0 \text{ for k=2,3} \tag{15}$$

$$\text{Consistency condition: } \beta_k \dot{f}_k = 0 \text{ for k=2,3} \tag{16}$$

The plastic flow β_k can be determined from the consistency condition $\beta_k \dot{f}_k = 0$ for k=2,3

$$\dot{f} = n \cdot q = n \cdot \dot{k_e}(\dot{v} - \dot{v}_p) \tag{17}$$

After substitution of the flow rule for $\dot{v}_p = n\beta$:

$$\dot{f} = n \cdot k_e(\dot{v} - n\beta) \tag{18}$$

From the consistency condition it is known that $\beta_k > 0$ only if $\dot{f}_k = 0$ for k=2,3 (α stands for active node, i.e., for a node with $\dot{f}_a = 0$:

$$\beta_a = \frac{(n_a^T k_e \dot{v})}{(n_a^T k_e n_a)} \tag{19}$$

The tangent modulus during plastic flow is:

$$k = k_e - \frac{k_e n_a n_a^T k_e}{(n_a^T k_e n_a)} \tag{20}$$

Below is given the summary of multi-surface plasticity for a linear elastic, perfectly plastic beam:

1. Additive deformation decomposition $v = v_e + v_p$
2. Force-deformation relation $q = k_e \cdot v_e = k_e \cdot (v - v_p)$
3. Yield condition $f(q_2, q_3) = n^T q - q_{pl} \leq 0$ with $n = [n_2 \quad n_3]$
4. Flow rule $\dot{v}_p = n_2\beta_2 + n_3\beta_3 = n\beta$ iff $f(q_2, q_3) = n^T q - q_{pl} = 0$
5. Kuhn – Tucker conditions $\beta_k \geq 0$ and $f_k \leq 0$ and $\beta_k f_k = 0$ for k=2,3
6. Consistency condition $\beta_k \dot{f}_k = 0$ for k=2,3

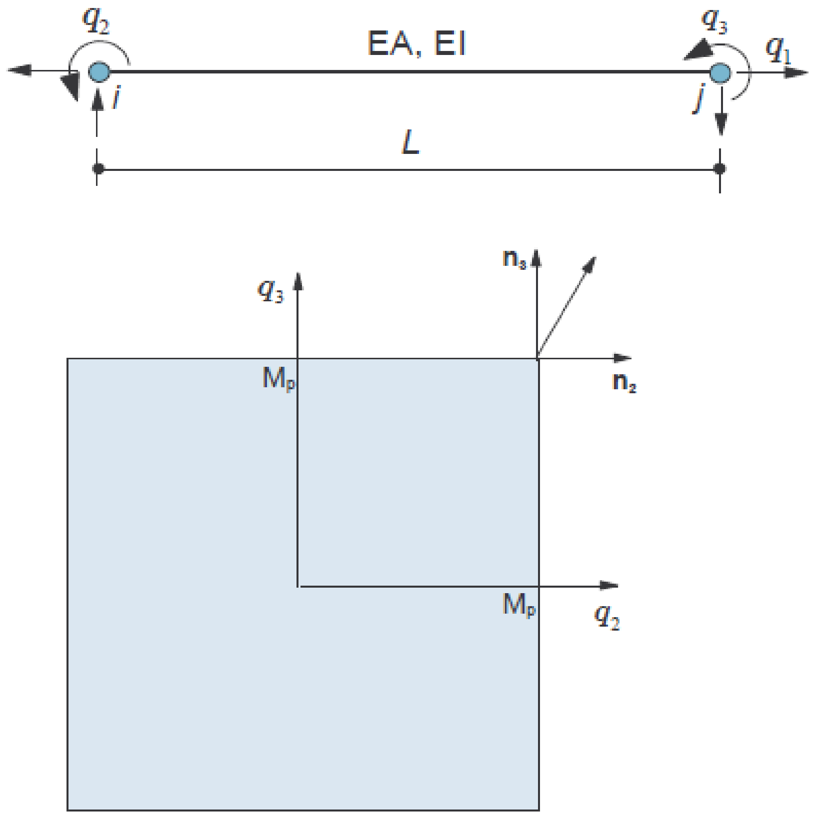

Figure 3. Linear elastic, perfectly plastic beam with non-smooth multi-surface plasticity (Filippou and Fenves 2004)

5. Correlation with experimental results

The experimental campaign (Petry and Beyer 2014) - employed in this numerical study - comprised five tests on masonry walls that all had the same dimensions (Height = 1.113 m, Length = 1.005 m, Thickness = 0.10 m). The walls were named PUM1–5. The moment, axial force and shear force at the top of the walls were introduced by three actuators (Figure 4). For these quasi-static cyclic tests, the five walls were constructed at each scale using the brick units and mortar that had been used for the material tests. More information about the material properties can be found in Petry and Beyer (2014). Each test stand allowed applying two vertical forces and one horizontal force. The control of the three actuators could be fully coupled. For each wall, the applied axial force and the shear span remained constant throughout the test.

In order to correlate with the above experimental results a MATLAB (MathWorks 2018) simulation code is developed. In Figure 4 this numerical model is also depicted. It is a cantilever configuration of each URM hollow clay brick wall with one-component frame model where the axial force is kept constant and equal to the experimental applied values (see Table 1) and the displacement history recorded at each wall (and transformed to the cantilever configuration) was imposed at the tip of the cantilever. The length of the cantilever for each URM wall is equal to the experimental shear span (see Table 1).

The correlation with the experimental results is depicted in Figure 5 for four out of five scaled URM hollow clay brick walls. It can be seen that the model can capture well the URM wall's initial stiffness, failure mode [KADET - shear failure (sliding, diagonal tension) or flexural failure] and maximum lateral strength. However, similar to bilinear models, this numerical model cannot represent the degradation of loading and unloading stiffnesses with increasing displacement amplitude reversals. Moreover, at high displacement amplitude the model deviates from the residual lateral strength of the URM wall due to extensive damage. Considering this, one proposal - for improvement of the correlation with the experimental results - could be to extend the formulation with a residual plastic moment when a building's Code (like KADET) specified deformation limit of the URM wall is exceeded or stop the analysis when the lateral force drops to 80% of the peak strength.

Table 1. Test Program, Petry and Beyer (2014)

Specimen	**Axial Force *N***	**Shear Span H_0**
PUM2	-105 kN	0.75H
PUM3	-105 kN	1.5H
PUM4	-155 kN	1.5H
PUM5	-55 kN	0.75H

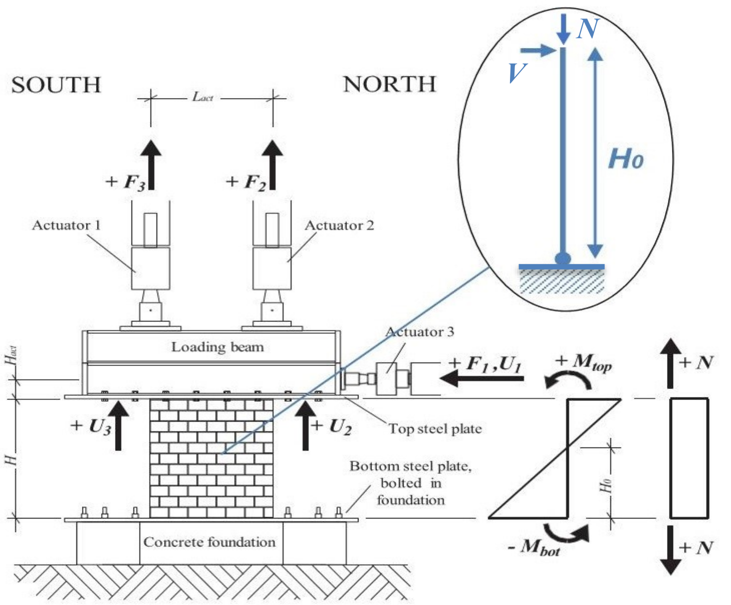

Figure 4. Experimental test setup (Petry and Beyer 2014) and numerical model of URM hollow clay brick walls

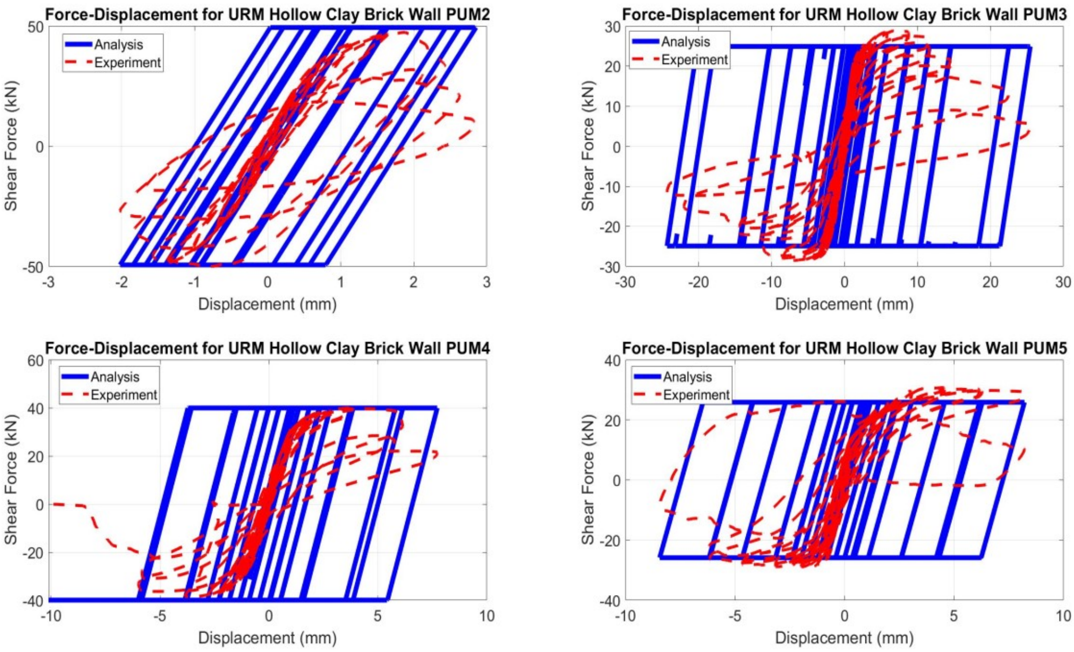

Figure 5. Correlation of the proposed one-component frame model of URM walls with the experimental results (Petry and Beyer 2014)

6. Discussion

In this study, similar to macro-elements simulating URM walls in recent literature, a concentrated plasticity beam model is proposed that can explicitly address accurately the principal failure modes of URM piers observed during experiments and included in Building Codes such as KADET. Moreover, such elements as the one proposed are readily available in many commercial programs and could be easily extended for simulating URM walls both for nonlinear pushover analysis but also for nonlinear time-history analysis of equivalent frame models of URM buildings. Beyond the scope of this study but necessary for future research would be to compare the analysis results of equivalent frame models of URM buildings using macro-elements with those based on the beam model proposed here. One aspect that is a privilege of one-component beam model proposal and a future research goal is that similar to in-plane behaviour of URM pier, its out-of-plane behaviour can also be modelled based on KADET with identical beam formulation. Finally, through the latter concept, an elastic 3D frame model can incorporate in the two loading lateral directions, separately and uncoupled, nonlinear plastic springs that simulate in-plane and out-of-plane behaviour of URM piers based on KADET.

7. Conclusions

To sum up, as demonstrated in recent earthquakes historical masonry buildings are highly vulnerable to seismic actions and therefore there is the need for simplified models and low-computation numerical methods to perform wide-area investigations.

To this end, based on the described approach in this study and on the results from the literature of an extensive experimental programme that included standard material tests and quasi-static cyclic tests on hollow clay brick URM walls subjected to horizontal and axial loads, a one-component frame model for URM walls' simulation under lateral cyclic excitation is proposed.

It is evident from the correlation with the employed experimental results that the model can capture adequately, the initial stiffness, failure mode (according to KADET) and maximum lateral strength under cyclic action of URM walls and could be further extended and adopted to the equivalent frame modelling of URM buildings based on KADET.

8. References

Ambra C.D., Lignola G., Prota A. (2016) Multi-scale analysis of in- plane behaviour of tuff masonry, Open Construct. Build. Technol. J, 89:312-328.

Bracchi S., Rota M., Penna A., Magenes G. (2015) Consideration of modelling uncertainties in the seismic assessment of masonry buildings by equivalent-frame approach, Bull. Earthquake Eng. 13(11):3423-3448.

Calderini C., Cattari S., Lagomarsino S. (2009) In-plane strength of unreinforced masonry piers, Earthquake Eng. Struct. Dynam., 38:243-267.

Cattari S., Camilletti D., D'Altri A. M., Lagomarsino S. (2021) On the use of continuum finite element and equivalent frame models for the seismic assessment of masonry walls. J Build Eng. 43: 102519.

Cattari S., Calderoni B., Caliò I., Camata G., de Miranda S., Magenes G., Milani G., Saetta A. (2022) Nonlinear modelling of the seismic response of masonry structures: critical aspects in engineering practice. Bull Earthq Eng 20:1939–1997.

Chen S.-Y., Moon F.L., Yi T. (2008) A macroelement for the nonlinear analysis of in-plane unreinforced masonry piers, Eng. Struct., 30(8):2242-2252.

DeJong M.J. (2009). Seismic assessment strategies for masonry structures, Ph.D. Thesis, Department of Architecture, Massachusetts Institute of Technology, Cambridge, Massachusetts, United States

Filippou, F. C., and Fenves, G. L. (2004) Methods of analysis for earthquake-resistant structures. In: Bozorgnia Y, Bertero VV (eds) Earthquake engineering: From engineering seismology to performance-based engineering. CRC Press, Boca Raton.

Giberson, M. F. (1967). The response of nonlinear multi-story structures subjected to earthquake excitation, Earthquake Engineering Research Laboratory, California Institute of Technology, Pasadena, CA, EERL Report.

Giberson, M.F. (1969) Two Nonlinear Beams with Definition of Ductility, Journal of Structural Division, ASCE, 95(ST2):137 - 157.

Hughes, T. J. R. (2000). The Finite Element Method: Linear Static and Dynamic Finite Element Analysis, Dover Publications.

James J, Kunnath S.K. (1994) Macroelement model for shear wall analysis. In: Proceedings of first congress on computing in civil engineering. p. 1505–12.

Kabeyasawa T, Shioara H, Otani S, Aoyama H. (1982) Analysis of the full-scale seven-story reinforced concrete test structure test PSD3. In: Proceedings of 3rd joint technical coordinate committee meeting.

Lagomarsino S., Penna A., Galasco A., Cattari S. (2013) TREMURI program: An equivalent frame model for the nonlinear seismic analysis of masonry buildings, Eng. Struct., 56:1787-1799.

Magenes G., Calvi G. (1996) Prospettive per la calibrazione di metodi semplificati per l'analisi sismica di pareti murarie, Atti del Convegno Nazionale La Meccanica delle murature tra teoria e progetto, Messina, pp. 18-20. [in Italian]

Marques R., Lourenço P. (2011) Possibilities and comparison of structural component models for the seismic assessment of modern unreinforced masonry buildings, Comp. Struct., 89:2079-2091.

Mathworks. (2018). MATLAB: User's Guide (r2018b).

Megalooikonomou KG, Parolai S, Pittore M. (2018) Toward performance-driven seismic risk monitoring for geothermal platforms: development of ad hoc fragility curves, Geothermal Energy Journal, 6(1):8

Petry S., Beyer K. (2014). Cyclic test data of five URM walls at half-scale [Data set]. In Bulletin of Earthquake Engineering 12(6):2557–2581. Zenodo. https://doi.org/10.5281/zenodo.12873

Pittore M., Haas M., Megalooikonomou KG. (2018) Risk-oriented, bottom-up modelling of building portfolios with faceted taxonomies, Frontiers in Built Environment, Section Earthquake Engineering. 4:41.

Regulation for Valuation and Structural Interventions for Masonry (KADET) (2022), Greece

Simo, J.C. and Hughes, T.J.R. (1998) Computational Inelasticity. Springer-Verlag, New York.